Progress In Electromagnetics Research, PIER 87, 215–231, 2008

ANALYSIS OF CYLINDRICALLY CONFORMAL MICROSTRIP STRUCTURES USING AN ITERATIVE METHOD

Y. Y. Wang, Y. J. Xie, and H. Feng

National Key Laboratory of Antennas and Microwave Technology
Xidian University
Xi'an, Shannxi 710071, P. R. China

Abstract—An efficient iterative method is presented for the fast analysis of cylindrically conformal microstrip structures. Based on the transmission line modeling (TLM) method and the fast modal transform (FMT) theory, this technique accelerates the process of the calculation by introducing the concept of the transverse electromagnetic waves instead of the transverse fields considered in the traditional algorithm. Within cylindrically stratified media, the transverse electromagnetic waves are represented by the hybrid modal basis functions. Ultimately, the specific form of the modal admittance and the spectral reflection matrix are deduced. Furthermore, the surface electric fields and electric currents of the cylindrically conformal microstrip antenna fed by means of a microstripline are calculated via the iterative process. On this basis, the input impedance of the antenna can also be obtained. And the results gained by utilizing iterative approach are compared with those from the published references to demonstrate the accuracy or efficiency of this method.

1. INTRODUCTION

Recent years, cylindrically conformal microstrip antennas [1–7] find more and more applications to various high-speed aircrafts, such as missiles, airplanes and satellites. Several models have been used to analyze this type of microstrip antennas. Among them, generalized transmission line model [3] and cavity model [4], as the earliest approximate models, are reasonable in considering some simple structures, but not accurate enough when the substrate is not very thin or there exists more intricate configurations. Besides, many kinds of numerical methods are also employed. When using the

method of moments (MoM) [8], the computation of the boring Green's functions [9–14] for cylindrically stratified media are inevitable, and the slowly convergent basis functions lead to a large calculation time. For the finite elements method (FEM) [15], a great number of cells are needed to simulate the whole spatial structures and amount of memory are taken up.

Based upon the transmission line modeling (TLM) method and the transverse electromagnetic wave theory, a novel iterative method is first introduced by H. Baudrand and has been successfully used for analyzing the planar microstrip circuits [16–18]. By extended to cylindrical coordinate system, this efficient method solved the scattering problem of metallic cylindrical aperture [19, 20] and the mutual coupling between slot antennas on a conducting cylinder [21]. Similarly, the scattering problems by arbitrarily shaped structures in free space or thin dielectric layer coated conductors have also been studied in [22] and [23], respectively. However, the iterative approach adopted to cylindrically conformal microstrip structures, which involve more complicated electromagnetic characteristics, is still worthy studying.

Differing from the planar case, there are neither pure TE_{nm} nor TM_{nm} polarized waves in cylindrical microstrip structures. And the hybrid modes results in a full spectral reflection matrix rather than a diagonal matrix for the decoupled case as the planar circuits.

It should be known that the cylindrical aperture or the slot antenna on metallic cylinder contains only one kind of waves in a region, which means that the standing waves and the travelling waves will not exist together on the inner or outer side of the interface. Thus the simple basis functions can provide satisfaction. Nevertheless, the selection of modal basis functions for the cylindrical microstrip structures seems much more difficult owing to the presence of standing waves together with travelling waves in the same substrates. Moreover, the functions must fulfil the electromagnetic field boundary conditions on each cylindrical interface.

In this article, considering the wave concept iterative process for planar microstrip circuits, an efficient iterative method suitable for calculating cylindrical microstrip structures is proposed. The theory as well as the detailed procedure is described in Section 2. Correspondingly, the scattering matrix, modal admittances and spectral reflection coefficients are also derived. To obtain a more precise equivalent circuit model, multiform modal basis functions are applied for expressing the transverse electromagnetic waves in dielectric medium layer. In Section 3, this technique is attested to be excellent via a comparison with method of moments. And in

Section 4, the numerical results are given and compared with those of the published literature [5] for illuminating the accuracy and the high efficiency of the iterative process. A time dependence $e^{j\omega t}$ is assumed and suppressed throughout this paper.

2. THEORY

The iterative method replaces the transverse fields or electric currents concerned in the traditional numerical algorithm with the transverse electromagnetic waves and its whole procedure crosses the spatial domain and the spectral domain.

In the first instance, the interfaces should be defined according to the structures being investigated. Generally speaking, the planes between two dielectric layers are chosen as the interface for the planar microstrip circuits. Analogously, the cylindrical interfaces are selected while taking account of the cylindrically conformal microstrip structures.

Secondly, the interfaces are divided into quadrangular pixels and their operations on the incident waves are depicted through the spatial-domain scattering matrix. Then the remaining half space is characterized as the equivalent mode transmission line and represented by the modal reflection matrix, which governs the spectral scattered waves coming from the interfaces. The iterative process is constructed via a multiple reflection procedure, which contains three main parts: initial conditions, the spatial-domain scattering and the spectral-domain reflecting. The connection between the spatial domain and spectral domain is carried out via the fast modal transform (FMT) [16]. A legible description of the iteration is illustrated in Fig. 1.

2.1. The Definition of the Transverse Waves

In accordance with the transmission line theory, the transverse incident and reflected waves can be denoted by the linear combinations of the transverse electric fields and currents:

$$\begin{cases} \vec{A}_i = \dfrac{1}{2\sqrt{Z_{0\mathrm{i}}}}\left(\vec{E}_i + Z_{0\mathrm{i}}\vec{J}_i\right) \\ \vec{B}_i = \dfrac{1}{2\sqrt{Z_{0\mathrm{i}}}}\left(\vec{E}_i - Z_{0\mathrm{i}}\vec{J}_i\right) \end{cases} \tag{1}$$

where $\vec{J}_i = \vec{H}_i \times \vec{n}_i$ and the subscripts indicate the different regions separated by the interfaces with $\vec{n}_i$ being the outgoing unit vector normal to the interface. $Z_{0\mathrm{i}}$ is the characteristic impedance of the medium i $(i = 1, 2)$.

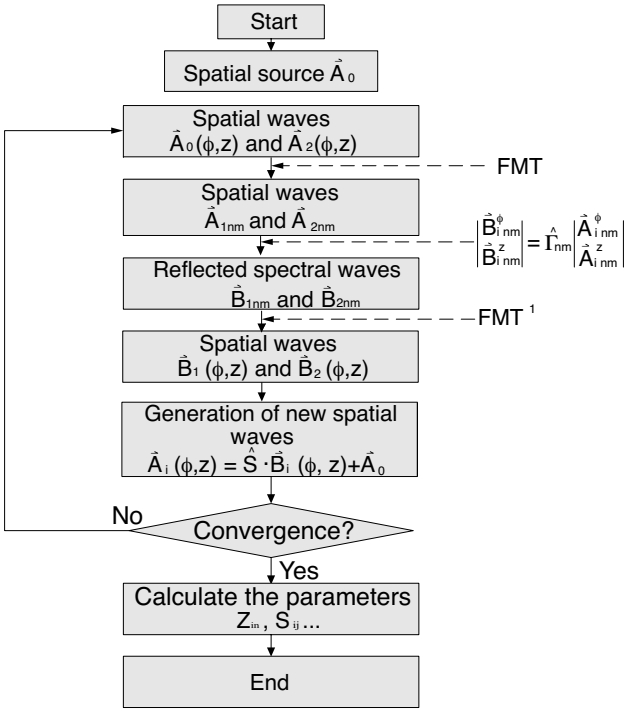

Figure 1. The iterative process.

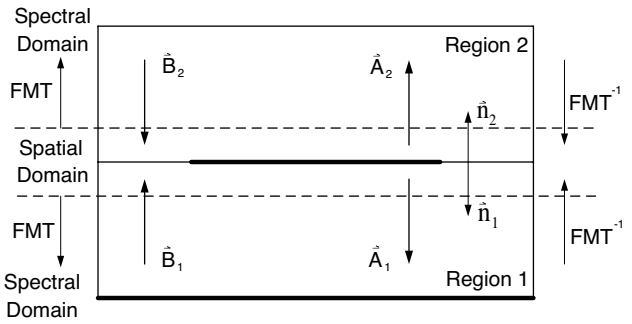

Figure 2. Scatter and reflection on the interface.

2.2. The Scattering Operator in Spatial Domain

Referring to Fig. 2, the interfaces scatter the waves $\vec{B}_i$ in the spatial domain as follows:

$$\vec{A}_i = \hat{S}\vec{B}_i \tag{2}$$

The scattering operator $\hat{S}$ is formed as a two-dimension matrix, whose elements correspond to the quadrangular cells on the interface. $\hat{S}$ can be obtained by matching the boundary conditions in each segment and all the segments would be classified into several different sorts: the dielectric domain, the metal domain (the metallic patch) and the source domain (the feeding part). Herein, we denote the functions H_d, H_m and H_s to indicate the three different domains, respectively. It is noticeable that the above functions equal to one in the relevant domain and zero elsewhere.

Because the electromagnetic boundary conditions hold true for any coordinate system, the scattering matrix for the cylindrical microstrip structures is therefore the same with that for the planar microstrip circuits as follows [17]:

$$\hat{S}=\begin{bmatrix} -H_m+\frac{1-N^2}{1+N^2}H_d+\frac{-1+n_1-n_2}{1+n_1+n_2}H_s & \frac{2N}{1+N^2}H_d+\frac{2m_1}{1+n_1+n_2}H_s \\ \frac{2N}{1+N^2}H_d+\frac{2m_1}{1+n_1+n_2}H_s & -H_m+\frac{N^2-1}{1+N^2}H_d+\frac{-1-n_1+n_2}{1+n_1+n_2}H_s \end{bmatrix} \tag{3}$$

where $N=\sqrt{\frac{Z_{01}}{Z_{02}}}$, $n_1=\frac{Z_0}{Z_{01}}$, $n_2=\frac{Z_0}{Z_{02}}$ and $m_1=\frac{Z_0}{\sqrt{Z_{01}Z_{02}}}$. $Z_0=\frac{Z_{01}\cdot Z_{02}}{Z_{01}+Z_{02}}$ is the equivalent impedance across the interface.

In each step of the iterative process, the outward waves $\vec{A}_i$ will be generated by the scattered waves $\hat{S}\vec{B}_i$ and the outgoing source waves $\vec{A}_{0\mathrm{i}}$:

$$\vec{A}_i=\hat{S}\vec{B}_i+\vec{A}_{0\mathrm{i}} \tag{4}$$

The source waves $\vec{A}_{0\mathrm{i}}$ could be given in the following form:

$$\vec{A}_{0\mathrm{i}}=\begin{pmatrix} \frac{E_\phi^0}{\sqrt{Z_{0\mathrm{i}}}} \\ \frac{E_z^0}{\sqrt{Z_{0\mathrm{i}}}} \end{pmatrix} \tag{5}$$

In (5), the material forms of the initial exciting electric fields E_ϕ^0 or E_z^0 lie on the configuration of the model.

2.3. The Reflection Operator in Spectral Domain

When considering the cylindrical microstrip structures, the two half spaces partitioned by the interface are equivalent to different modal

transmission lines and the admittance matrix $\hat{Y}_{\mathrm{i}\,nm}$ [24] connected to the Green's functions is also defined in the spectral domain as follows:

$$\begin{bmatrix} J^{\varphi}_{\mathrm{i}\,nm} \\ J^{z}_{\mathrm{i}\,nm} \end{bmatrix} = \hat{Y}_{\mathrm{i}\,nm} \begin{bmatrix} E^{\varphi}_{\mathrm{i}\,nm} \\ E^{z}_{\mathrm{i}\,nm} \end{bmatrix} = \begin{bmatrix} Y^{11}_{\mathrm{i}\,nm} & Y^{12}_{\mathrm{i}\,nm} \\ Y^{21}_{\mathrm{i}\,nm} & Y^{22}_{\mathrm{i}\,nm} \end{bmatrix} \begin{bmatrix} E^{\varphi}_{\mathrm{i}\,nm} \\ E^{z}_{\mathrm{i}\,nm} \end{bmatrix} \tag{6}$$

With the discontinuous tangential components of the magnetic field, one can obtain the elements of the admittance matrix $\hat{Y}_{\mathrm{i}\,nm}$ on either side of the interface and the expressions of the spectral admittance coefficients are detailed in appendix. Then the spectral reflection matrix is represented by the admittance matrix as follows:

$$\hat{\Gamma}_{\mathrm{i}\,nm} = \left(\bar{I} - Z_{0\mathrm{i}}\hat{Y}_{\mathrm{i}\,nm}\right)\left(\bar{I} + Z_{0\mathrm{i}}\hat{Y}_{\mathrm{i}\,nm}\right)^{-1} \tag{7}$$

where $\bar{I}$ is the identity matrix and the subscripts n, m denote the modes indices in the $\hat{\varphi}$ direction and $\hat{z}$ direction, respectively. Expanding Equation (7) and simplifying it, we can obtain the spectral reflection coefficients as follows:

$$\hat{\Gamma}_{nm} = \frac{1}{D_{nm}} \begin{bmatrix} \Gamma^{11}_{nm} & \Gamma^{12}_{nm} \\ \Gamma^{21}_{nm} & \Gamma^{22}_{nm} \end{bmatrix} \tag{8}$$

where

$$\begin{aligned} D_{nm} &= 2 + Z_0\left(Y^{11}_{nm} + Y^{11}_{nm}\right) \\ \Gamma^{11}_{nm} &= -\Gamma^{22}_{nm} = Z_0\left(Y^{22}_{nm} - Y^{11}_{nm}\right) \\ \Gamma^{12}_{nm} &= \Gamma^{21}_{nm} = -2Z_0 Y^{12}_{nm} \end{aligned}$$

It is worthy of note that the TE_{nm} and TM_{nm} modes are not coupled in the case of the planar microstrip but coupled for the cylindrical microstrip. So the more complex reflection matrices ought to be reasonable for the cylindrical multilayer structures. Especially for the cylindrical dielectric substrate, the standing waves exist as well as the outgoing travelling waves. This phenomenon makes the simple modal basis functions [21] disabled and the new kinds of hybrid modal basis functions taking full account of the two different waves will be elaborated in the next section.

2.4. The Modal Basis Functions

The operations in the spatial domain and spectral domain are given in 2.2 and 2.3, respectively.

$$\begin{cases} \vec{A}_i = \hat{S}\vec{B}_i + \vec{A}_0 & \text{spatial domain} \\ \vec{B}_{\mathrm{i}\,mn} = \hat{\Gamma}_{\mathrm{i}\,mn}\vec{A}_{\mathrm{i}\,mn} & \text{spectral domain} \end{cases} \tag{9}$$

To implement the iterative process, the two parts in Equation (9) can be linked by the fast modal transform (FMT) and its inverse (IFMT):

$$A_i(\varphi, z) \overset{FMT}{\longrightarrow} A_{\mathrm{i}\,mn} = \iint_s A_i(\varphi, z) \cdot f^*_{\mathrm{i}\,mn}(\varphi, z)\, ds \tag{10}$$

$$B_{\mathrm{i}\,mn} \overset{IFMT}{\longrightarrow} B_i(\varphi, z) = \sum_n \sum_m B_{\mathrm{i}\,mn} f_{\mathrm{i}\,mn}(\varphi, z) \tag{11}$$

where the modal basis functions $f_{\mathrm{i}\,nm}$ are the solutions of the cylindrical Helmoltz's equation in region i, which have the periodicity along the axial direction or the azimuthal direction and can be written as the combinations of the standing waves containing the first-kind Bessel functions and the outgoing waves represented by the second-kind Hankle functions. Because there are no boundary conditions imposed in the free space out of the interface, which has a radius b, the basis functions are formulated in the form of travelling waves:

$$f_{2nm} = \frac{1}{\sqrt{2\pi bd}} e^{-jn\varphi} e^{-jk_m z} \frac{H_n^{(2)}(k_{2\rho}\rho)}{H_n^{(2)}(k_{2\rho}b)} \tag{12}$$

With (10) and (11), the transformation in the exterior space can be completed. In contrary, the basis functions should consider either the travelling or the standing waves inside the interface. Besides, the basis functions also satisfy the transverse electric fields boundary conditions on the surface of the inner conductor. Nevertheless, it is so difficult for the single basis functions as in (12) to describe the characteristics comprehensively or exactly that the electric fields and the magnetic fields are figured by different functions as in (13) and (14), respectively, which are derived from the vectorial wave equation and fulfill the boundary conditions in the substrate region. Then the combined hybrid basis functions will be made up in accordance with the Equation (1).

$$f^e_{1nm} = \frac{1}{\sqrt{2\pi\, bd}} e^{-jn\varphi} e^{-jk_m z} \left[\frac{J_n(k_{1\rho}\rho)}{H_n^{(2)}(k_{1\rho}\rho)} - \frac{J_n(k_{1\rho}a)}{H_n^{(2)}(k_{1\rho}a)} \right] \tag{13}$$

$$f^h_{1nm} = \frac{1}{\sqrt{2\pi\, bd}} e^{-jn\varphi} e^{-jk_m z} \left[\frac{J_n(k_{1\rho}\rho)}{H_n^{(2)}(k_{1\rho}\rho)} - \frac{J'_n(k_{1\rho}a)}{H_n^{(2)'}(k_{1\rho}a)} \right] \tag{14}$$

In (12)–(14), $J_n(x)$ and $J'_n(x)$ are the n-order bessel function and its derivative, respectively. $H_n^{(2)}(x)$ and $H_n^{(2)'}(x)$ are the n-order Hankel function of the second kind and its derivative, which denote

the travelling waves. The radii of the inner metallic cylinder and the interface on which the patch is laying are a and b. The model structure has a distance d along the z-direction. As the propagation constant along the ρ-direction, $k_{i\rho}$ will be written as:

$$k_{i\rho} = \begin{cases} \sqrt{\left|\varepsilon_{ri}k_0^2 - k_m^2\right|} & \sqrt{\varepsilon_{ri}}k_0 \geq k_m \\ -j \cdot \sqrt{\left|\varepsilon_{ri}k_0^2 - k_m^2\right|} & \sqrt{\varepsilon_{ri}}k_0 < k_m \end{cases} \tag{15}$$

where $k_m = 2\pi\, m/d$ is the propagation constant along the z-direction and the k_0 is wave number in the free space. Considering the calculating efficiency, the mode indices m, n are presented identical with the number of the segments in the φ and z directions. Then the high-order modes (larger than the number of the segments) could be neglected and this assumption is proved in practice.

3. ANALYSIS OF THE EFFICIENCY

As the link between the two different domain, FMT and FMT^{-1} avoid the inversion of the large matrix, save the computer's memory and accelerate the operation prominently. Unlike the common numerical methods, this iterative algorithm has the complexity proportional to the size of the interface without regard to the detailed configurations on it.

For demonstrating the advantages of the method in this paper, the complexity of iterative method is compared with that of the MoM. We can assume that: P is the amount of the segments on the interface; N represents the number of the iterations and K denotes the scale of the metallic part. In general, the overall complexities are $N_T = N\left(4P + 12P\ln P\right)$ for the iterative method and $\left(KP\right)^3/3$ for the MoM. Taking no account of the troublesome Green's functions needed in the Method of moments, the iterative process behaves more excellent when the parameters fulfil the condition: $N_T = N\left(4P + 12P\ln P\right) < \left(KP\right)^3/3$. And the more distinct results are illustrated as follows:

From the figures above, it is realized that the more the segments or the metallic parts are, the more efficient and superior the iterative method is. For the condition of 64×64 cell, the iterative process always converges below 500 steps and the iterative method excels the MoM all the while. The troublesome and time-consuming computing of the slow-convergent cylindrically stratified green' functions decelerate the calculation when using the MoM.

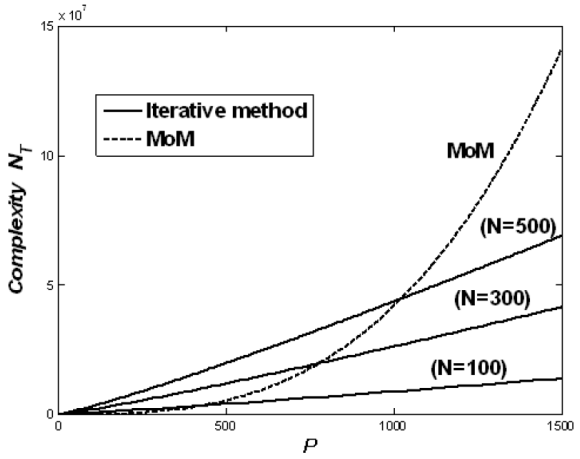

Figure 3. The complexities of the WCIP and the MoM ($K = 0.5$).

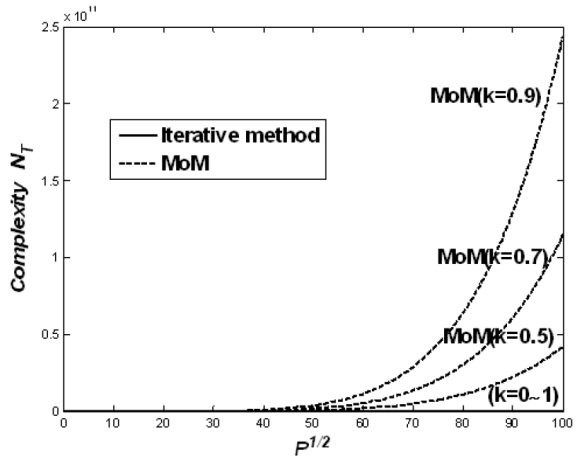

Figure 4. The complexities of the WCIP and the MoM ($N = 500$).

4. NUMERICAL RESULTS

To demonstrate the approach in this paper, we consider the cylindrically conformal microstrip antennas [5] fed by microstriplines. The structures are supposed to be invariant along the axial direction of the cylinder. As shown in Fig. 5, the radii of the inner conducting cylinder and the air-dielectric interface are $r_1 = 2.5\,\text{cm}$ and $r_2 = 2.659\,\text{cm}$ respectively. Note that the substrate has a dielectric

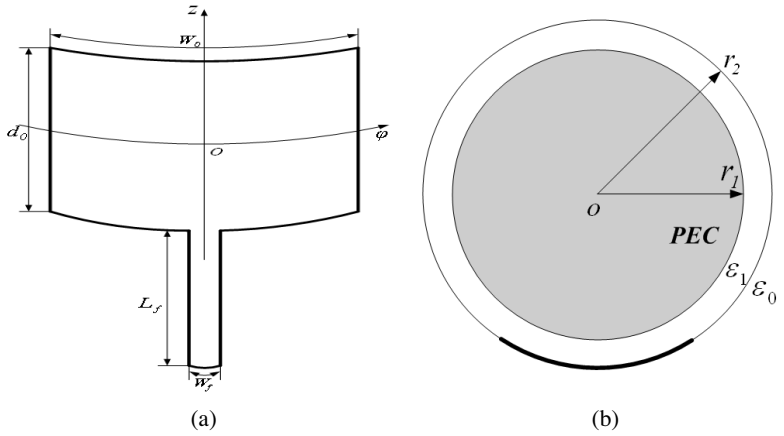

(a) (b)

Figure 5. The structure of the cylindrically conformal microstrip antenna: (a) the metallic patch, (b) the cylindrical structure.

permittivity $\varepsilon_1 = 2.57\varepsilon_0$, where ε_0 is the dielectric permittivity in the vacuum and both of the regions have the magnetic permeability μ_0. The dimension of the rectangular patch is $W_0 = d_0 = 4.02\,\text{cm}$ with that of the feeding line $W_f = 0.477\,\text{cm}$ and $L_f = \lambda_1/2$, where λ_1 is the guided wavelength along the line.

According to the parameters of the structure, the cylindrical interface will be divided into 64×64 quadrangles and the size of the corresponding spatial scattering matrix is 64×64 either. Herein,we define the initial excitation in equation (5) as the exponential functions, which can be derived via the electric currents appeared in reference [5]. For enhancing the velocity of the FMT, the number of the quadrangles is usually chosen as 2^n. At the qth iteration, we can derive the expressions of the surface electric currents and fields as follows:

$$\begin{cases} \vec{E}_i^q = \sqrt{Z_{0\text{i}}}\left(\vec{A}_i^q + \vec{B}_i^q\right) \\ \vec{J}_i^q = \dfrac{1}{\sqrt{Z_{0\text{i}}}}\left(\vec{A}_i^q - \vec{B}_i^q\right) \end{cases} \tag{16}$$

Through 500 iterations, the surface electric fields and the surface electric current density along the $\hat{\varphi}$-direction and $\hat{z}$-direction are available in Fig. 6 and Fig. 7 at the frequency point 2.25 GHz. Because the width of the transmission line W_f is far smaller than the wavelength, so it is logical that the $\hat{\varphi}$-direction electric currents seem scarce along the feeding line as shown in Fig. 7(a).

After finishing the iterative process, the input impedance and the

input admittance can be attained via the surface electric currents and the surface electric fields on the cells of the source domain. Fig. 8 presents the normalized input admittance as the function of the number of the iterations at 2.25 GHz. It can be seen that the

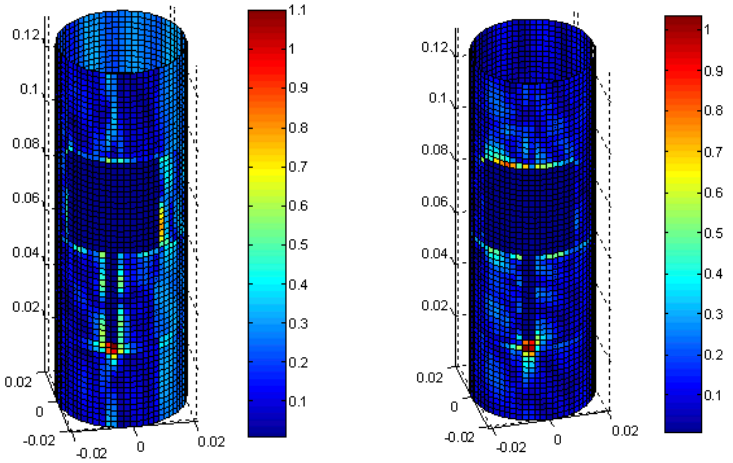

Figure 6. (a) The $\hat{\varphi}$-direction surface electric fields. (b) The $\hat{z}$-direction surface electric fields.

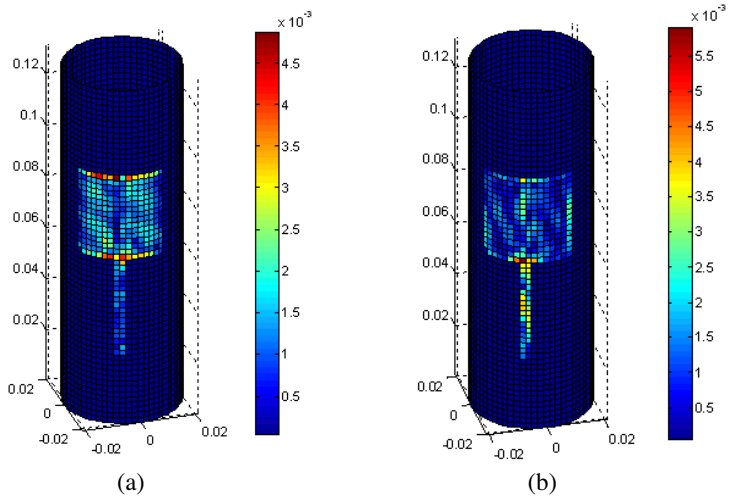

Figure 7. (a) The $\hat{\varphi}$-direction surface electric current density. (b) The $\hat{z}$-direction surface electric current density.

convergence, which is judged by an error of 0.05, has been achieved after the 250th step. Because the modulus of the modal coefficients of the reflection matrix is less than unity, the convergence of the iteration is thus always ensured.

Figure 9 shows the curves of the normalized input impedance of the cylindrically conformal microstrip antenna. For each frequency point, the calculation costs 10.2 seconds by 500 iterations. Although there exists a little frequency shift, the results obtained via the iterative approach agree quite well with that have been published in [5] using the MoM.

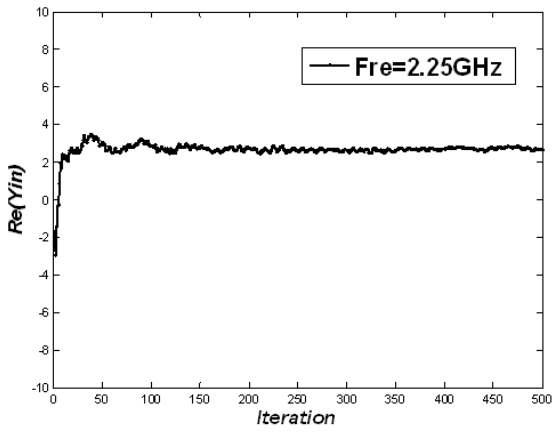

(a)

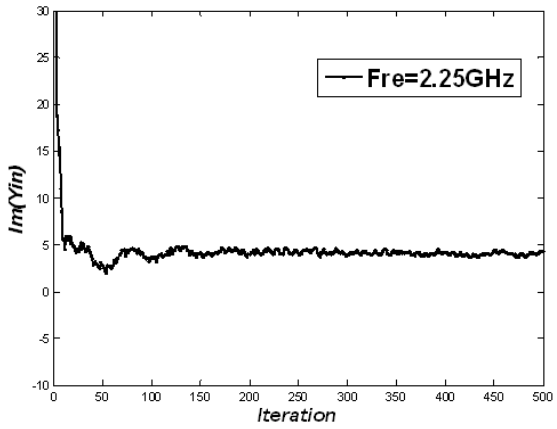

(b)

Figure 8. Convergence curves for the normalized input admittance: (a) real part, (b) imaginary part.

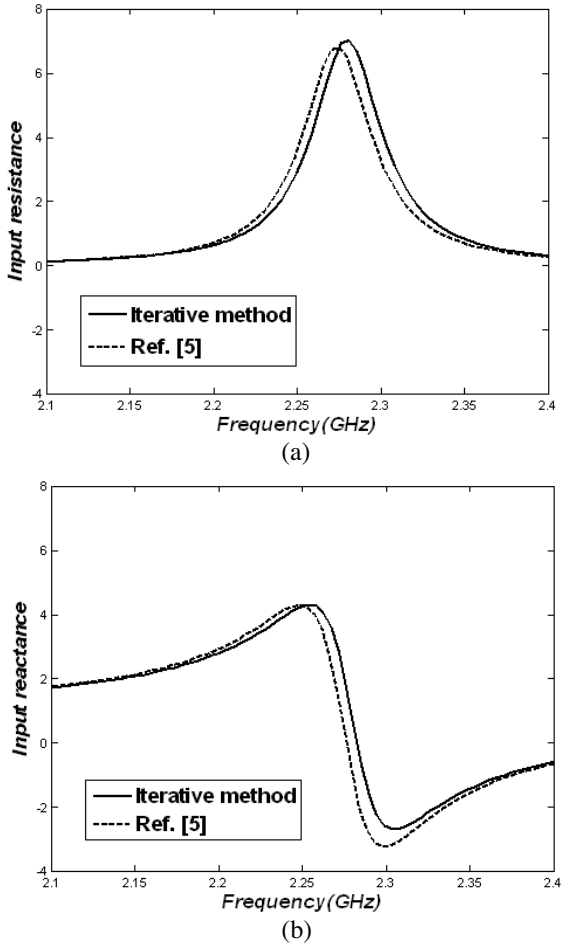

Figure 9. The normalized input impedance calculated by the WCIP and MoM: (a) input resistance, (b) input reactance.

The precision of the calculation can be enhanced by employing more meshing cells on the interface or more high-order modal components in the spectral domain. The former means more storage for conserving the larger matrices, while the latter indicates longer computational time for dealing with the high-order special functions.

5. CONCLUSIONS

Based on the reported iterative technique for planar microstrip circuits, we have presented an efficient iterative approach for calculating the cylindrically conformal microstrip structures. In cylindrical microstrip structures, the spectral reflection matrix has been deduced as well as the hybrid mode basis functions which are developed for describing the waves in dielectric substrate. Owing to the adoption of the fast modal transform (FMT), the time-consuming matrix operations and the numerous computations of the cylindrical green's functions are avoided. Consequently, this iterative approach economizes the memory and quickens the process of the analysis. In conclusion, the proposed method is validated through a published example and the good agreements between the simulation results and the published results are observed.

APPENDIX A.

Considering the vectorial wave equation in cylindrical coordinate system, the transverse components of the magnetic fields could be denoted by the transverse electric fields. From the general solutions of the axial fields, we can obtain the spectral admittance matrices inside and outside the cylindrical interface as follows:

1. Outside the Interface

$$\hat{Y}_{nm_{out}} = \begin{bmatrix} Y^{11}_{nm_{out}} & Y^{12}_{nm_{out}} \\ Y^{21}_{nm_{out}} & Y^{22}_{nm_{out}} \end{bmatrix} \tag{A1}$$

Where

$$Y^{11}_{nm_{out}} = \frac{k_{2\rho}}{j\omega\mu_0} \frac{H^{(2)}_n(k_{2\rho}b)}{H^{(2)'}_n(k_{2\rho}b)} \tag{A2}$$

$$Y^{12}_{nm_{out}} = Y^{21}_{nm_{out}} = \frac{-jnk_m}{\omega\mu_0 bk_{2\rho}} \frac{H^{(2)}_n(k_{2\rho}b)}{H^{(2)'}_n(k_{2\rho}b)} \tag{A3}$$

$$Y^{22}_{nm_{out}} = \frac{j\omega\varepsilon_0}{k_{2\rho}} \frac{H^{(2)'}_n(k_{2\rho}b)}{H^{(2)}_n(k_{2\rho}b)} + \frac{k_{2\rho}}{j\omega\mu_0} \left(\frac{nk_m}{bk^2_{2\rho}}\right)^2 \frac{H^{(2)}_n(k_{2\rho}b)}{H^{(2)'}_n(k_{2\rho}b)} \tag{A4}$$

2. Inside the Interface: The Region of the Substrate

$$\hat{Y}_{nm_{in}} = \begin{bmatrix} Y^{11}_{nm_{in}} & Y^{12}_{nm_{in}} \\ Y^{21}_{nm_{in}} & Y^{22}_{nm_{in}} \end{bmatrix} \tag{A5}$$

where

$$Y_{nm_{in}}^{11} = -\frac{k_{1\rho}}{j\omega\mu_0}\frac{r^{(h)}}{\beta_1} \tag{A6}$$

$$Y_{nm_{in}}^{12} = Y_{nm_{in}}^{21} = \frac{jnk_m}{\omega\mu_0 bk_{1\rho}}\frac{r^{(h)}}{\beta_1} \tag{A7}$$

$$Y_{nm_{in}}^{22} = -\frac{j\omega\varepsilon_1}{k_{1\rho}}\cdot\beta_1\cdot r^{(e)} - \frac{k_{1\rho}}{j\omega\mu_0}\left(\frac{nk_m}{bk_{1\rho}^2}\right)^2\frac{r^{(h)}}{\beta_1} \tag{A8}$$

$$r^{(e)} = \frac{\xi_2-\eta_1}{\eta_2-\eta_1} \quad r^{(h)} = \frac{\eta_2-\xi_1}{\xi_2-\xi_1} \tag{A9}$$

$$\eta_1 = \frac{H_n^{(2)}(k_{1\rho}a)}{J_n(k_{1\rho}a)}, \quad \eta_2 = \frac{H_n^{(2)}(k_{1\rho}b)}{J_n(k_{1\rho}b)}$$

$$\xi_1 = \frac{H_n^{(2)'}(k_{1\rho}a)}{J_n'(k_{1\rho}a)}, \quad \xi_2 = \frac{H_n^{(2)'}(k_{1\rho}b)}{J_n'(k_{1\rho}b)} \tag{A10}$$

$J_n(x)$ and $J_n'(x)$ are the n-order bessel function and its derivative, respectively. $H_n^{(2)}(x)$ and $H_n^{(2)'}(x)$ are the n-order hankel function of the second kind and its derivative.

ACKNOWLEDGMENT

This work was supported by program for New Century Excellent Talents in University (NECT-04-0950).

REFERENCES

1. Habashy, T. M., S. M. Ali, and J. A. Kong, "Input impedance and radiation pattern of cylindrical-rectangular and wraparound microstrip antennas," *IEEE Trans. Antennas Propagat.*, Vol. 38, No. 5, 722–731, May 1990.
2. Cooray, F. R. and J. S. Kot, "Analysis of radiation from a cylindrical-rectangular microstrip patch antenna loaded with a superstrate and an air gap using the electric surface current mode," *Progress In Electromagnetics Research*, PIER 67, 135–152, 2007.
3. Wong, K. L., Y. H. Liu, and C. Y. Huang, "Generalized transmission line model for cylindrical-rectangular microstrip

antenna," *Microwave and Optical Technology Letters*, Vol. 7, No. 16, 729–732, Jan. 1994.

4. Luk, K. M., K. F. Lee, and J. S. Dahele, "Analysis of the cylindrical-rectangular mictrostrip patch antenna," *IEEE Trans. Antennas Propagat.*, Vol. 37, No. 21, 143–147, Feb. 1989.
5. Franklin, F. C., S. B. A. Fonseca, J. M. Soares, and A. J. Giarola, "Analysis of microstrip antennas on circular-cylindrical substrates with a dielectric overlay," *IEEE Trans. Antennas Propagat.*, Vol. 39, No. 9, 1398–1403, Sept. 1991.
6. Svezhentsev, A. Y., "Some far field features of cylindrical microstrip antenna on an electrically small cylinder," *Progress In Electromagnetics Research B*, Vol. 7, 223–244, 2008.
7. Erturk, V. B. and R. G. Rojas, "Efficient analysis of input impedance and mutual coupling of microstrip antennas mounted on large coated cylinders," *IEEE Trans. Antennas Propagat.*, Vol. 51, No. 4, 739–749, Apr. 2003.
8. Harrington, R. F., *Field Computation by Moment Methods*, Macmillan, New York, 1968.
9. Tokgöz, C. and G. Dural, "Closed-form Green's functions for cylindrically stratified media," *IEEE Trans. Microwave Theory and Tech.*, Vol. 48, No. 1, 40–49, Jan. 2000.
10. Sun, J., C.-F. Wang, L.-W. Li, and M. -S. Leong, "Mixed potential spatial domain Green's functions in fast computational form for cylindrically stratified media," *Progress In Electromagnetics Research*, PIER 45, 181–199, 2004.
11. Acar, R. C. and G. Dual, "Mutual coupling of printed elements on a cylindrically layered structure using closed-form Green's functions," *Progress In Electromagnetics Research*, PIER 78, 103–127, 2008.
12. Sun, J., C.-F. Wang, L.-W. Li, and M.-S. Leong, "A complete set of spatial-domain dyadic Green's function components for cylindrically stratified media in fast computational form," *Journal of Electromagnetic Waves and Applications*, Vol. 16, No. 11, 1491–1509, 2002.
13. Li, L.-W., S. B. Yeap, M.-S. Leong, T.-S. Yeo, and P.-S. Kooi, "Eigenfunctional representation of dyadic Green's functions in cylindrically multilayered gyroelectric chiral media," *Progress In Electromagnetics Research*, PIER 42, 143–171, 2003.
14. Li, L.-W., M.-S. Leong, T.-S. Yeo, and P.-S. Kooi, "Electromagnetic dyadic Green's functions in spectral domain for multilayered cylinders," *Journal of Electromagnetic Waves and Applications*,

Vol. 11, No. 7, 961–986, July 2000.

15. Silvester, P. P. and R. L. Ferrari, *Finite Elements for Engineering*, Cambridge University Press, Cambridge, U.K., 1990.
16. Titaouine, M., A. G. Neto, H. Baudrand, and F. Djahli, "WCIP method applied to active frequency selective surfaces," *Journal of Microwave and Optoelectronics*, Vol. 6, No. 1, 1–16, June 2007.
17. Hajiaoui, E. A., H. Trabeisi, H. Zairi, A. Gharsallah, and H. Baudrand, "Analysis of multilayer substrates by multilayer contribution of wave concept itrative process," *Microwave and Optical Technology Letters*, Vol. 49, No. 6, 1439–1445, June 2007.
18. Mami, A., H. Zairi, A. Gharsallah, and H. Baudrand, "Analysis of microstrip spiral inductor by using iterative method," *Microwave and Optical Technology Letters*, Vol. 35, No. 4, 302–306, Nov. 2002.
19. Raveu, N., T. P. Vuong, I. Terrasse, G.-P. Piau, and H. Baudrand, "Near fields evaluated with the wave concept iterative procedure method for an E-polarisation plane wave scattered by cylindrical strips," *Microwave and Optical Technology Letters*, Vol. 38, No. 5, 403–406, Sept. 2003.
20. Bdour, T., N. Ammar, T. Aguili, and H. Baudrand, "Modeling of wave penetration through cylindrical aperture using an iterative method based on transverse wave concept," *IEEE Microwave Conference KJMW*, 45–48, 2007.
21. Raveu, N., T. P. Vuong, I. Terrasse, G.-P. Piau, G. Fontgalland, and H. Baudrand, "Wave concept iterative procedure applied to cylinders," *IEE Proceedings, Microwave, Antennas and Propagation*, Vol. 151, No. 5, 409–416, Oct. 2004.
22. Ammar, N., T. Bdour, T. Aguili, and H. Baudrand, "Investigation of electromagnetic scattering by arbitrarily shaped structures using the wave concept iterative process," *Journal of Microwaves, Optoelectronics and Electromagnetic Applications*, Vol. 7, No. 1, 26–43, June 2008.
23. Bedira, R., A. Gharsallah, L. Desclos, A. Gharbiand, and H. Baudrand, "The wave concept iterative process: Scattering of a conducting target coated by a thin dielectric layer," *AP-Symposium*, Vol. 2, 98–101, 2002.
24. Harrington, R. F., *Time-harmonic Electromagnetic Fields*, McGraw-Hill, New York, 1961.